

Conceptual design of a 20T High Field Dipole Magnet

Lorenzo Andrea Parrotta

September 26, 2014

Mentor: Dr. Emanuela Barzi, FNAL

*Superconducting R&D
Magnet System Department
Fermilab Technical Division.*

Contents

1	Introduction	4
2	Coil and cables geometry	4
I	An analytical model for <i>cosine-θ</i> type magnets	4
3	General hypotheses	5
4	Magnetic model	5
4.1	Hypoteses	5
4.2	Complete Magnetic Field Expression	5
5	Mechanical model	6
5.1	Hypoteses	6
5.2	Stress Field	7
5.3	Load boundary conditions	8
6	Field Quality requirements and optimization	8
6.1	An explicative example	8
7	First step: 1T HTS insert within an existing 11T Nb_3Sn dipole coil	11
7.1	Loadline	11
7.2	Stress field in the coil	12
8	Second Phase: 5T HTS within a 15T Nb_3Sn dipole coil	13
9	Conclusions and remarks	17

Abstract

FNAL goal for next future will be the development of very high field accelerator magnets beyond the limits of Nb_3Sn technology, based on combination of the Low Temperature Superconductors (LTS) and High Temperature Superconductors (HTS) coils. This work tries to understand the main aspects of a mechanical design of such magnets, taking into account superconducting material limits and design requirements.

1 Introduction

In recent years the quest for higher field in particle accelerator magnets became crucial for future discoveries of new particles and interactions. In this scenario the development of new materials and technologies for present and future accelerators is one of Fermilab's core competencies. After the obsolescence of $Nb - Ti$ technology and the present maturity of Nb_3Sn cables, a new class of superconducting material starts to be investigated. The HTS (High Temperature Superconductors) appear to be suitable for future accelerator magnets due to their higher critical density current curve for high fields. The upgrading strategies are *current density* grading and *material* grading. The main advantage of the first one is a considerable decrease of the amount of conductor needed, as well as coil size and costs. The second possibility consists in placing less performing material in the low field region. For magnets above $10 - 15T$ one can then imagine hybrid coils and HTS inserts within Nb_3Sn outer coils. Next generation of accelerators will hopefully see Nb_3Sn coils pushed towards their theoretical limit of $15T$ field with $5T$ HTS coil inserts, in order to approach $20T$ bore fields.

Another issue concerns the materials used for HTS superconductors. Two generations of conductors are currently available: $1G$ of $BSCCO - 2212$ round wires and $2G$ $YBCO$ tapes. $2G$ HTS present higher density current limits, but on the other side they exhibit a strong angular anisotropy.

The strategy to achieve this cutting-edge goal passes through different phases. This study develops a general model to analyze stress and strain fields inside the coil, in order to evaluate the coil working conditions and to understand the feasibility of the solutions proposed. The first step in this process will be to realize and test a $1T$ HTS insert within an existing $60mm$ aperture $11T$ dipole. Then, a $15T + 5T$ magnet was taken into consideration.

Special attention was dedicated only to dipole coils in this work.

2 Coil and cables geometry

Accelerator specifications require constant fields inside the bore for accelerator dipoles. There are many possibilities to achieve the constant field requirement. The *cosine- θ* dipoles consist of a sector coil made of superconducting strands. The latter are wound following the magnet's major length around a central bore (where the particle beam is supposed to pass).

The cables used for Nb_3Sn and $BSCCO - 2212$ magnets are the so called *Rutherford* cables, each made of n round wires.

The current flowing through the conductors arrangement makes it possible to obtain the magnetic field desired.

The coils are surrounded with clamps or *collars*, providing the precise coil geometry and the pre-stress needed for good performance at high field. Then, an Iron Yoke screens the fringe field outside the magnet and provides field contribution to the magnet.

Part I

An analytical model for *cosine- θ* type magnets

3 General hypotheses

Simplicity criteria and trade-offs are used to develop the present model, in order to obtain useful results for magnet design. The analysis must take into account magnetic field, stress and strain fields inside the coil and boundary conditions for coil blocks.

The analysis is subdivided into two different parts, the first one approaching the Magnetic Fields generated by superconducting cables and the second building a Mechanical Model for coil blocks. After that, Field Quality requirements are taken into account. Then, the model is used to study two different cases: 1T HTS insert within an existing 11T Nb_3Sn dipole coil; 5T HTS within a 15T Nb_3Sn dipole coil.

Symmetry allows limiting the analysis to only one quarter of the problem, that is the first quarter if a reference system placed in the bore center is considered

4 Magnetic model

4.1 Hypoteses

Under the circumstances of current conductors running parallel to the beam over the longest part of the magnet except for the short coil ends, one can consider the magnetic field essentially as two-dimensional and apply the theory of analytic functions.

Current shell distributions are considered for the model and higher multipole terms are neglected. Yoke magnetic effects are neglected for this preliminary study.

4.2 Complete Magnetic Field Expression

The field \mathbf{B} can be expressed as the curl of the vector potential \mathbf{A} :

$$\mathbf{B} = \nabla \times \mathbf{A}$$

For the two-dimensional hypothesis \mathbf{A} has only a z component: $\mathbf{A} = A_z \hat{k}$. The r and θ components can be computed as:

$$B_\theta = -\frac{\partial A_z}{\partial r} \quad B_r = \frac{1}{r} \frac{\partial A_z}{\partial \theta}$$

One can observe that in a coil with dipole symmetry, for four line currents, the vector potential becomes:

$$\left\{ \begin{array}{l} A_z(r, \theta) = \frac{2\mu_0 I}{\pi} \sum_{n=1,3,5..} \frac{1}{n} \left(\frac{a}{r}\right)^n \cos(n\theta) \cos(n\phi), \quad r > a \\ A_z(r, \theta) = \frac{2\mu_0 I}{\pi} \sum_{n=1,3,5..} \frac{1}{n} \left(\frac{r}{a}\right)^n \cos(n\theta) \cos(n\phi), \quad r < a \end{array} \right.$$

Considering a coil sector cross section with coil angle ϕ_l and thickness w , and assuming constant density current on the section ($I = J \int a \, da \, d\theta$), the previous expressions will be integrated for three different regions:

- for $r < a$, inside the aperture;
- for $a < r < a + w$, on the coil;
- for $r > a$, in order to take into account \mathbf{B} generated by the coil on the outer region.

The results are presented below:

$$\begin{cases} A_z(r, \theta) = \frac{2\mu_0 J_0}{\pi} w r \cos(\theta) \sin(\phi_l), & r < a \\ A_z(r, \theta) = \frac{2\mu_0 J_0}{\pi} r \left[(a + w - r) + \frac{r^3 - a^3}{3r^2} \right] \cos(\theta) \sin(\phi_l), & a < r < a + w \\ A_z(r, \theta) = \frac{2\mu_0 J_0}{\pi} r \left[\frac{r^3 - a^3}{3r^2} \right] \cos(\theta) \sin(\phi_l), & r > a. \end{cases}$$

A vectorial representation of the Magnetic Field is given in figure 1.

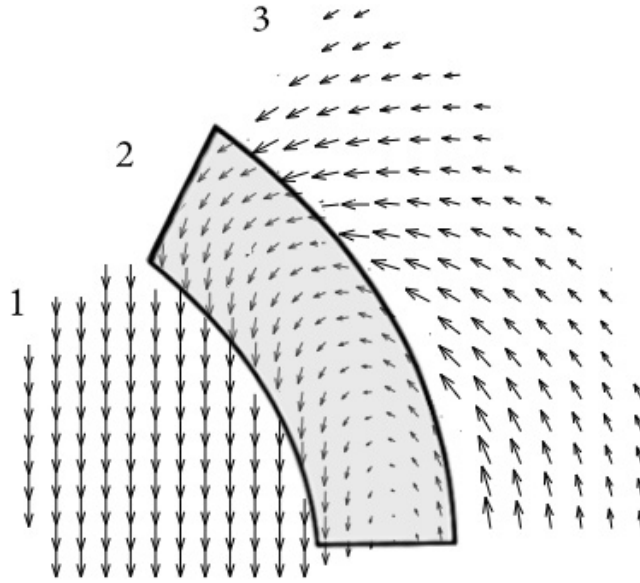


Figure 1

5 Mechanical model

5.1 Hypotheses

With the underlying hypotheses of 2-D model and Linear, Elastic, Omogeneous and Isotropic material, the mechanical model chosen to analyze the coil block is a thick membrane sector. No thermal effects are considered.

5.2 Stress Field

Using the notation displayed in picture, the equilibrium equations for a membrane sector element in cylindrical coordinates can be written:

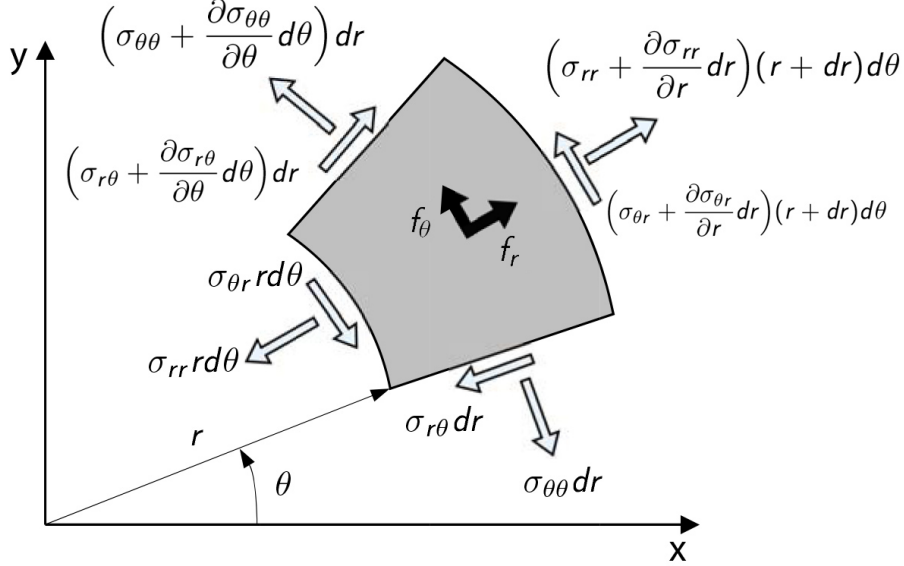


Figure 2: Membrane element with forces acting on it

$$\begin{cases} \frac{\partial \sigma_{rr}}{\partial r} + \frac{\sigma_{rr} - \sigma_{\theta\theta}}{r} + \frac{1}{r} \frac{\partial \sigma_{r\theta}}{\partial \theta} + f_r = 0 \\ \frac{1}{r} \frac{\partial \sigma_{\theta\theta}}{\partial \theta} + \frac{\partial \sigma_{r\theta}}{\partial r} + 2 \frac{\sigma_{r\theta}}{r} + f_\theta = 0 \end{cases}$$

For an outward current density J_0 :

$$f_\theta(r, \theta) = -B_\theta(r, \theta) J_0 = J_0 \frac{\partial A_z(r, \theta)}{\partial r}$$

$$f_r(r, \theta) = B_r(r, \theta) J_0 = J_0 \frac{1}{r} \frac{\partial A_z(r, \theta)}{\partial \theta}$$

Based on previous studies (Bologna), a generalized plain strain model is considered. The generalized plain strain theory allows calculating the axial stress as follows:

$$\sigma_{zz} = \nu(\sigma_{rr} + \sigma_{\theta\theta}) - \overline{\sigma_{zz}},$$

where:

$$\overline{\sigma_{zz}} = \frac{1}{\pi[(a+w)^2 - a^2] \frac{(\phi_2 - \phi_1)}{2\pi}} \int_{\phi_1}^{\phi_2} \int_a^{a+w} \sigma'_{zz} r \, dr d\theta,$$

being $\overline{\sigma_{zz}}$ and σ'_{zz} the average axial stress and the axial stress for $\epsilon_{zz} = 0$.

In order to solve the equations for a structure with multiple coils, the sum of vector potential contributions from each coil having an effect on the one considered must be taken into account. Furthermore, shear stress was neglected for the two directions to obtain an analytical solution for the problem.

5.3 Load boundary conditions

Load boundary conditions are shown in picture for two different cases: the first for a standalone dipole (having its own mechanical structure) and the second for a structure made of different coils (no friction is supposed).

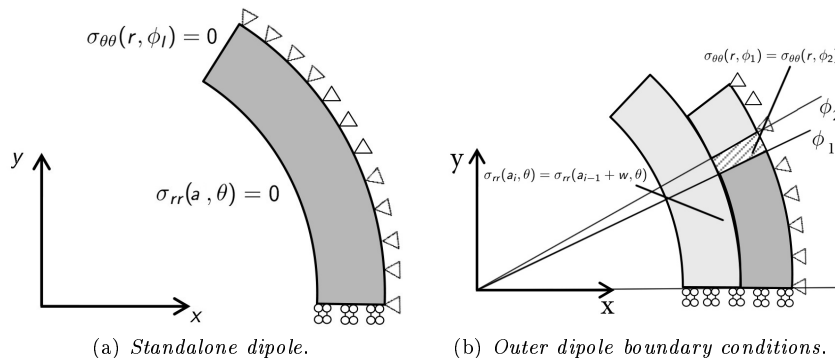


Figure 3: Load Boundary Conditions

6 Field Quality requirements and optimization

Particle accelerator magnets require high fields with good field quality. The latter is defined by the number of multipoles allowed after the magnet's design and construction. In fact, the real magnet approximates the $\cos(\theta)$ distribution by means of current shells with sufficient accuracy. The quality of the approximation can be judged from the general multipole expansion.

The complex magnetic field can be expanded in the multipole series:

$$B_y + iB_x = B_{ref} \sum_{n=1}^{\infty} (b_n + ia_n) \left(\frac{x + iy}{r_0} \right)^{n-1},$$

where r_0 is a reference radius, the quantity B_{ref} is a reference field, for instance the magnitude of the main field at the reference radius and a_n , b_n are the multipole coefficients. The a_n are called *skew* coefficients and they are cancelled by symmetry, while the b_n are the *normal* coefficients. They depends on sectors' geometry, including sector angles and wedges.

Since for a sector starting at ϕ_1 and ending at ϕ_2 with internal radius a and thickness w results:

$$b_n \propto (\sin(n\phi_2) - \sin(n\phi_1)) \left(\frac{1}{a^{n-2}} - \frac{1}{(a+w)^{n-2}} \right), \quad n = 3, 5, 7, 9, \dots,$$

one could write a system whose unknown are $\phi_1, \phi_2, \dots, \phi_n$ (placing various sectors and wedges) in order to make b_1, b_2, \dots, b_n vanishing.

6.1 An explicative example

In order to acquire awareness of how magnetic field optimization is not only helpful, but also necessary for magnet design a simple exercise can be analyzed,

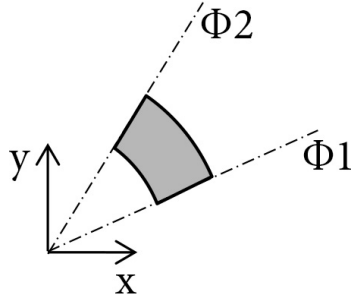


Figure 4: Coil sector

in which two configurations are compared: the configuration *I* with four coil sectors optimized in order to make normal multipole coefficients vanishing until b_9 ; the configuration *II* consisting in one 60° block. Both the configurations have the same internal radius $a = 30\text{mm}$ and the same current density is chosen to be $800 \frac{\text{A}}{\text{mm}^2}$.

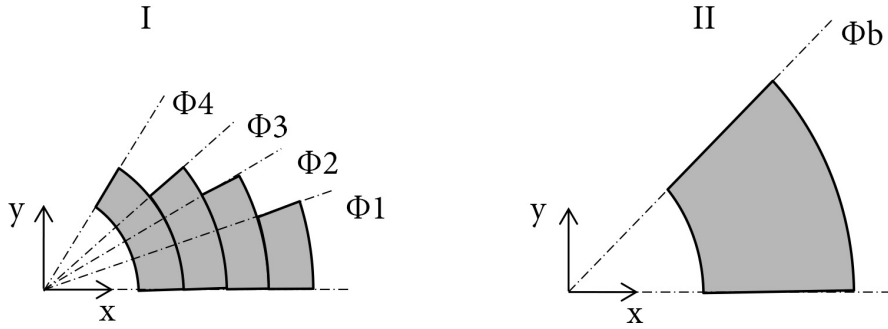


Figure 5: Two coil structures compared

The other geometrical properties are presented in the table below:

ϕ_1	20°
ϕ_2	46°
ϕ_3	57°
ϕ_4	78°
ϕ_b	60°
$w_{sector,I}$	$0.19a$
w_b	$4w_i$

The two configurations share the same total thickness, too.

The results of the analysis are first of all in terms of normal multipole coefficients:

	<i>I</i>	<i>II</i>
b_3	0	0
b_5	0	$-4 \cdot 10^{-3}$
b_7	0	$5 \cdot 10^{-4}$
b_9	0	0
b_{11}	$5 \cdot 10^{-6}$	$-1 \cdot 10^{-5}$

Then, the cross section surface and bore magnetic field ratios can be evaluated:

- $\frac{S_I}{S_{II}} = 0.269$
- $\frac{B_I}{B_{II}} = 0.834$.

So, with a small reduction of bore field generated, a strong material saving is achieved.

With the explained model stress field can be evaluated.

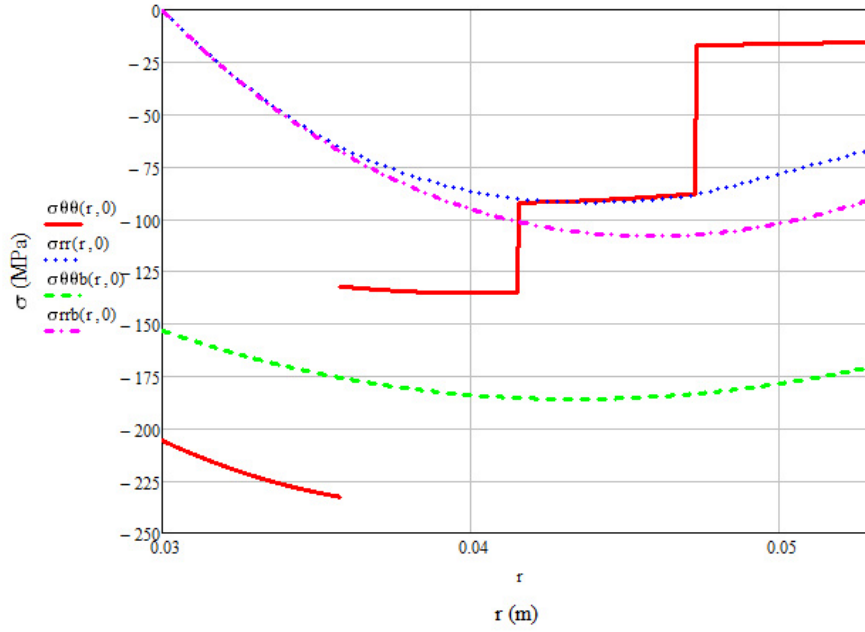


Figure 6: Subscript b indicates stress components for configuration *II*. Stress component for configuration *I* are indicated without subscript.

It shows that stress levels for multiple blocks configuration are lower, except for first Nb_3Sn sector.

7 First step: 1T HTS insert within an existing 11T Nb_3Sn dipole coil

For this first step a standalone *BSCCO* HTS insert with only a single 60 degrees sector is considered. The insert will fit inside an existing 60mm 11T dipole.

7.1 Loadline

The electromagnetic model provides at this point the so-called *loadlines*, i.e. the relation current density versus peak field on the coil. HTS current density J increases starting from a background field of about 11T generated by outer dipole. Then, the working conditions in terms of J depends on the critical current density curve. The intersection of the loadline with the critical surface provides the maximum performance of the magnet. Obviously, a margin is needed. For this case it could be achieved with a $J_{0,HTS}$ of about $300A/mm^2$, which gives the magnetic field desired.

The other parameters are presented in the table below:

a	15 mm
w	5 mm
J_{0,Nb_3Sn}	$800 \frac{A}{mm^2}$

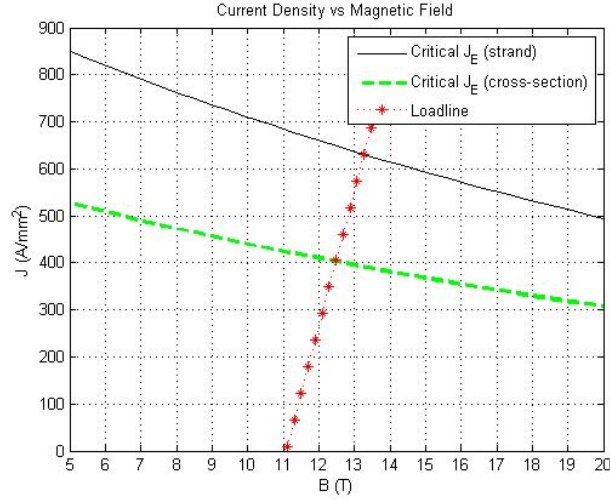


Figure 7: HTS insert loadline in 11T background field

Critical Engineering Current Density for *Bi – 2212* strand was taken from *Fermilab* experimental data. Then, Critical Engineering Current Density for coil cross section is calculated taking into account voids between the 0.8mm round strands and 0.05mm of insulation around each strand, yielding:

$$J_{E,section} = J_{E,strand} \frac{\frac{\pi}{4} d^2}{(d + 2t)^2}.$$

7.2 Stress field in the coil

Solving equilibrium equation with the hypothesis of neglecting shear stress leads to the stress field in the coil. Lorentz forces represent the volume forces f_r and f_θ for the coil sector. The contribution of the outer dipole as well as its self contribution must be taken into account for calculating the vector potential $A_z(r, \theta)$.

The results for σ_{rr} , $\sigma_{\theta\theta}$ and σ_{zz} are shown in figure 8.

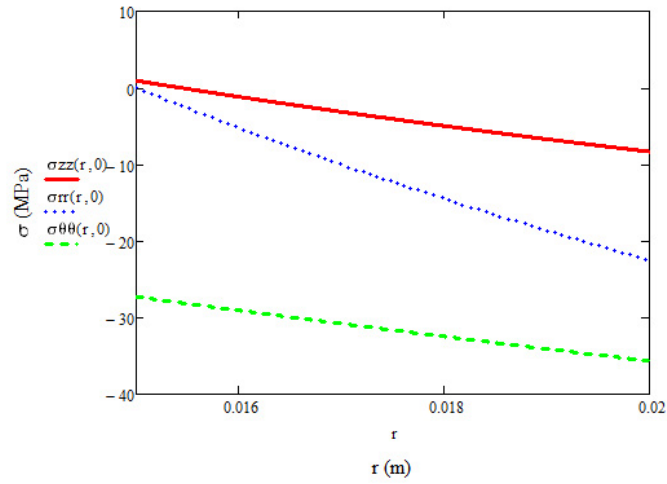


Figure 8

Then, the Von Mises equivalent stress is calculated and presented in figure 9.

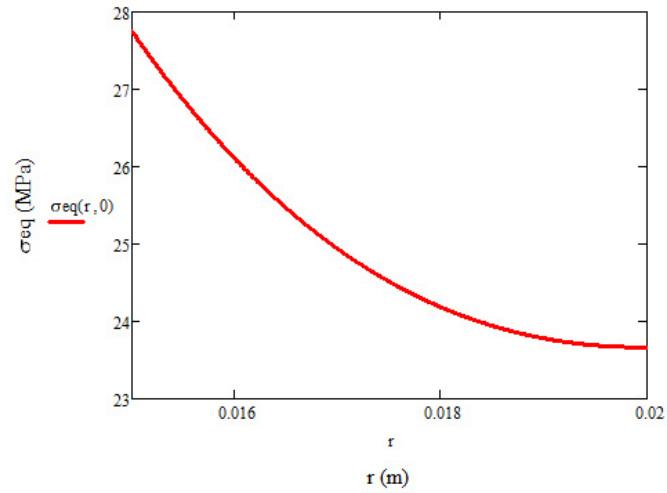


Figure 9

Then, from Stress Field, Strain Field can be evaluated by means of consti-

tutive equations:

$$\begin{pmatrix} \epsilon_{rr} \\ \epsilon_{\theta\theta} \end{pmatrix} = \frac{1}{E} \begin{bmatrix} 1 - \nu^2 & -\nu(1 + \nu) \\ -\nu(1 + \nu^2) & 1 - \nu^2 \end{bmatrix} \begin{pmatrix} \sigma_{rr} \\ \sigma_{\theta\theta} \end{pmatrix} + \frac{\nu}{E} \overline{\sigma_{zz}}$$

$$\epsilon_{zz} = -\frac{\overline{\sigma_{zz}}}{E}.$$

Strain field must be considered and compared with $Bi - 2212$ strain limits (present works are trying to clarify them).

8 Second Phase: 5T HTS within a 15T Nb_3Sn dipole coil

For this second phase a magnetic field quality optimization is performed on the magnet. Normal multipoles until b_9 were chosen to be cancelled. Separate optimization for HTS blocks and Nb_3Sn blocks are considered in this study, even if other optimization can be imagined (Few words will be spent later). For this reason a two sector configuration is chosen for HTS insert, having two blocks separated by one wedge in the first sector.

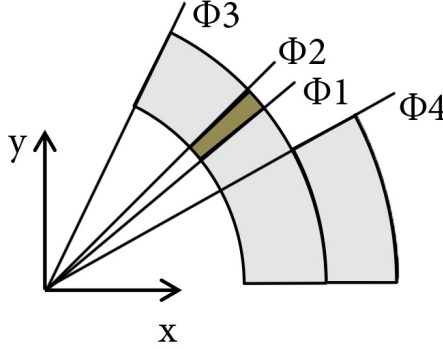


Figure 10: HTS blocks for the 5T magnet.

The system of equations for the field quality optimization is presented:

$$\begin{cases} [\sin(3\phi_1) - \sin(3\phi_2) + \sin(3\phi_3)] \left(\frac{1}{a} - \frac{1}{a+w} \right) + \sin(3\phi_4) \left(\frac{1}{a+w} - \frac{1}{a+2w} \right) = 0 \\ [\sin(5\phi_1) - \sin(5\phi_2) + \sin(5\phi_3)] \left(\frac{1}{a^3} - \frac{1}{(a+w)^3} \right) + \sin(5\phi_4) \left(\frac{1}{(a+w)^3} - \frac{1}{(a+2w)^3} \right) = 0 \\ [\sin(7\phi_1) - \sin(7\phi_2) + \sin(7\phi_3)] \left(\frac{1}{a^5} - \frac{1}{(a+w)^5} \right) + \sin(7\phi_4) \left(\frac{1}{(a+w)^5} - \frac{1}{(a+2w)^5} \right) = 0 \\ [\sin(9\phi_1) - \sin(9\phi_2) + \sin(9\phi_3)] \left(\frac{1}{a^7} - \frac{1}{(a+w)^7} \right) + \sin(9\phi_4) \left(\frac{1}{(a+w)^7} - \frac{1}{(a+2w)^7} \right) = 0. \end{cases}$$

Imposing the internal radius $a = 25mm$ and the thickness w along with the condition of a resulting bore field of 5T (at a certain $J_{0,HTS}$), the system could lead to a solution, found with the help of *MATLAB* solver.

The result of HTS optimization in terms of outer radius is then used as input for Nb_3Sn optimization.

$$a_{Nb_3Sn} = a_{HTS} + 2w_{HTS}$$

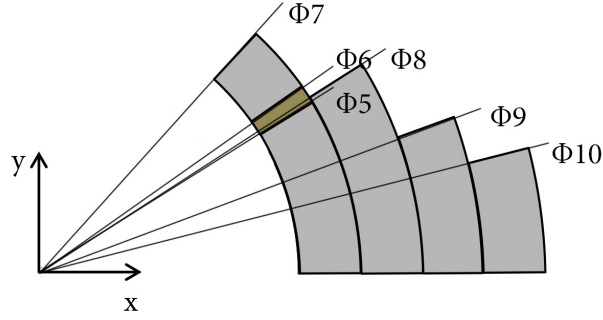


Figure 11: Nb_3Sn blocks for the 15T magnet.

Four coil sectors are considered, with two blocks in the first sector.

It leads to a system of 5 equations in 7 unknowns if current density J is chosen (unknowns are angles from ϕ_5 to ϕ_{10} and thickness -equal for each sector- w). Among the two free parameters, e.g. the wedge angular extension can be chosen equal to 5° . With these premises angles from ϕ_5 to ϕ_{10} are plotted against w/r_i ratio.

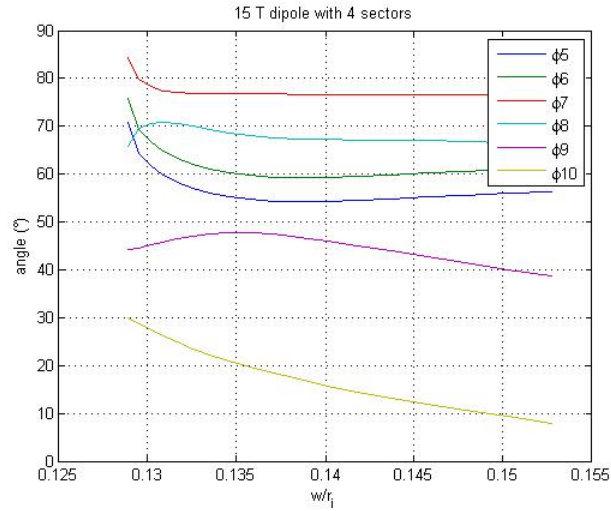


Figure 12: Angles ϕ_5 to ϕ_{10} vs w/r_i ratio.

Stress Field can be evaluated for the coil sectors using the mechanical model developed.

Looking at stress levels it is clear that these are not allowable both for insert sectors and outer dipole sectors. In fact, the HTS limits can be considered approximately close to $70MPa$, while Nb_3Sn stress levels must be taken below $165MPa$. Based on the distributions shown, a first attempt of mechanical structure design can be proposed and shown in figure 14. It is based upon the alternation of coil sectors and stainless steel shells, the latter characterized by a *slotted* configuration. The main idea is the presence of *structural wedges* linked to the shell, of fundamental importance in order to lower azimuthal stress levels

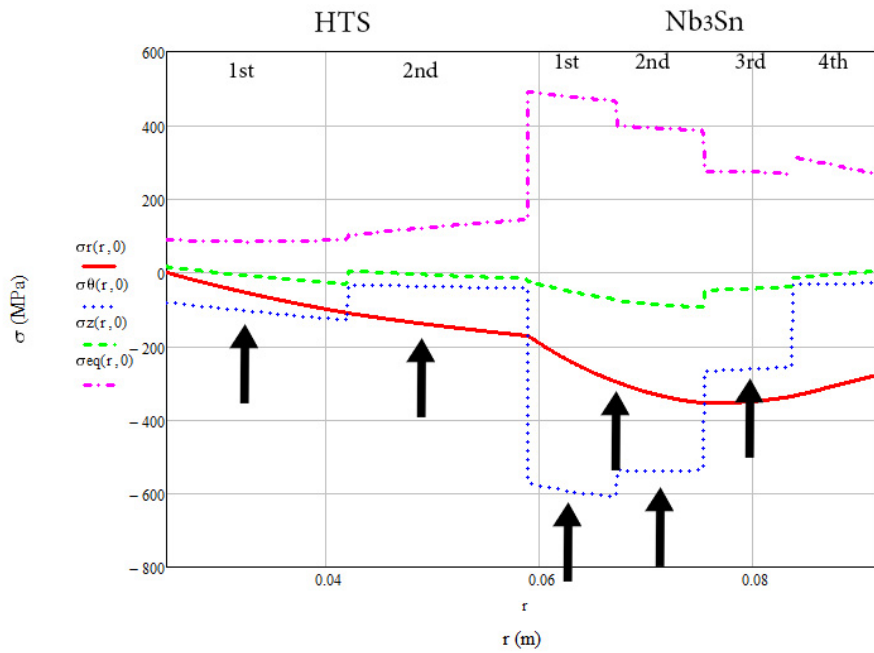


Figure 13: Stress levels on the coil sectors. σ_{eq} refers to Von Mises equivalent stress

on the sectors. The second Nb_3Sn sector was split for this reason into two blocks, adding another parameter to the optimization system.

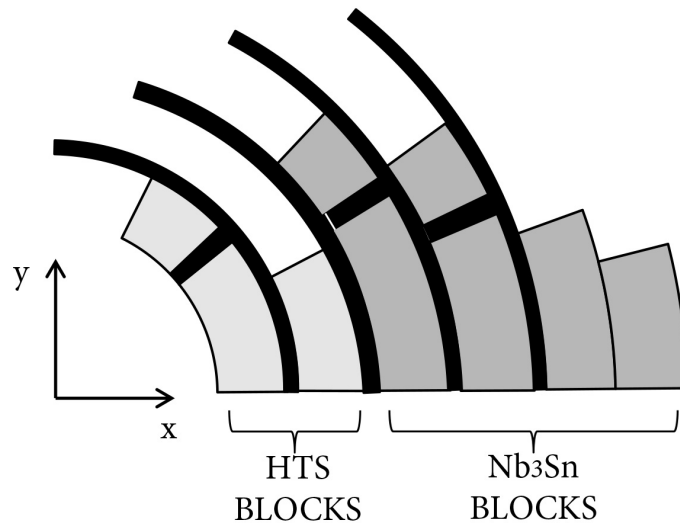


Figure 14: First design of a mechanical structure for the dipole (quarter of cross section represented)

At this point an optimization on the proposed structure must be done, in an iterative process going through Finite Element Method simulations, in order to find the best structure in terms of mechanical stresses although preserving field quality requirements.

For example, considering for the first shell a thickness of 3mm , the desired parameters (sector angles and thickness) of HTS blocks can be chosen based on wanted current density.

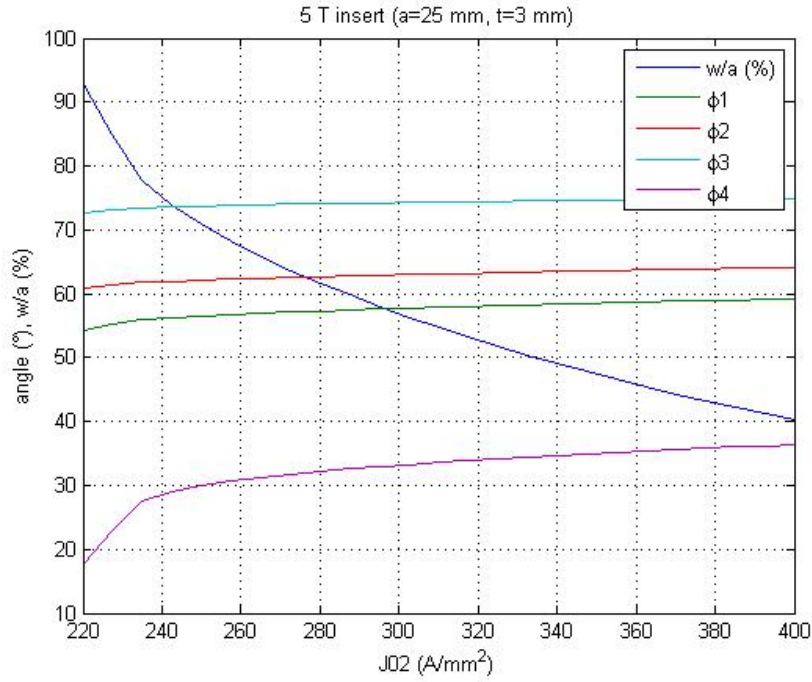


Figure 15: First design of a mechanical structure for the dipole

Other optimization strategies

Crossed optimization Other kinds of optimizations can be thought for the structure; in particular two must be considered. The first one can be called *crossed optimization*, and its main point is adding material in the regions of lower stress levels and compensate the multipoles arisen. For example, extra material can be added on the second *HTS* sector, obtaining an increased sector angle. This will lead to new optimal angles and at least $b_9 \neq 0$. At this point Nb_3Sn sectors can be used to compensate the lack of balance.

Total optimization The optimization strategy can be applied to the whole structure, thus considering all magnetic layers and sector angles. The result will be a multiparametric system, whose functions can be minimized, instead of being put to zero, with the help of specific algorithms.

9 Conclusions and remarks

The analysis done can be a good starting point for future magnet design, since it offers an overview of the working conditions of sector coils. Due to the simplifying hypotheses at the basis of the model, the results must be taken into account as first order estimates, for future FEM implementations. These preliminary results are anyway particularly important in engineering design, for let the designer making initial choices.

Some important points emerged, above all:

- an HTS $1T$ insert results feasible with state-of-the-art $Bi - 2212$ characterization (for stress and strain limits);
- the need for a strong stress management solution results for the final structure, and towards this direction the azimuthal stress management can be achieved by means of new *structural wedges*.

New samples of $BSCCO$ will be tested in TD in next future along with samples from $2G$ (YBCO) HTS superconductors. These last superconductors cannot be produced as Rutherford type cables. They are produced in tapes and are based instead on thin film approach, showing highly anisotropic behavior with respect with field orientation, which needs to be accounted for in magnet design. To give an idea, this could be exploited for an insert coil placing each tape according to local direction of total magnetic field for regime condition inside the outer dipole.

References

- [1] M. Danuso, 2008-2009 *"Study of electromechanical effects in high field accelerator magnets"*, Master Thesis in Mechanical Engineering, University of Pisa.
- [2] D. Turrioni, E. Barzi, M.J. Lamm, R. Yamada, A. V. Zlobin, A. Kikychi *"Study of HTS wires at High Magnetic Fields"*.
- [3] E. Terzini *"Analytical Study of Stress State in HTS solenoids"*, FERMILAB-TM-2448-TD.
- [4] K. Mess, P.Schmuser, S. Wolff, 1996 *"Superconducting Accelerator Magnets"*, World Scientific.